

Acceleration of the Discrete Green's Function Formulation of the FDTD Method Based on Recurrence Schemes

Jacek Gulgowski¹, Tomasz P. Stefański²,

¹The Faculty of Mathematics, Physics and Informatics, University of Gdansk, Gdansk, Poland,
jacek.gulgowski@mat.ug.edu.pl

²Faculty of Electronics, Telecommunications and Informatics, Gdansk University of Technology, Gdansk, Poland,
tomasz.stefanski@pg.edu.pl

Abstract—In this paper, we investigate an acceleration of the discrete Green's function (DGF) formulation of the FDTD method (DGF-FDTD) with the use of recurrence schemes. The DGF-FDTD method allows one to compute FDTD solutions as a convolution of the excitation with the DGF kernel. Hence, it does not require to execute a leapfrog time-stepping scheme in a whole computational domain for this purpose. Until recently, the DGF generation has been the limiting step of DGF-FDTD due to large computational resources, in terms of processor time and memory, required for these computations. Hence, we have derived the no-neighbours recurrence scheme for one-dimensional FDTD-compatible DGF using solely properties of the Gauss hypergeometric function (GHF). Using known properties of GHF, the recurrence scheme is obtained for arbitrary stable time-step size. In this paper, we show that using the recurrence scheme, computations of 1-D FDTD solutions with the use of the DGF-FDTD method can be around an order of magnitude faster than those based on the direct FDTD method. Although 2- and 3-D recurrence schemes for DGF (valid not only for the magic time-step size) still need to be derived, the 1-D case remains the starting point for any research in this area.

Index Terms—computational electromagnetics, Green's function methods, finite-difference time-domain methods.

I. INTRODUCTION

The discrete Green's function (DGF) is a kernel of the convolution computations that allows one to obtain the same solutions as those from the FDTD method [1]. Due to its promising properties, DGF is investigated for many years [2], [3], [4], [5], [6], [7], [8]. Contrary to the discretization of the continuous Green's function, DGF-based solutions have properties characterized by dispersion, anisotropy and stability properties of the FDTD method. Hence, it is identified that DGF can open new prospects for the hybridization of FDTD with the use of integral-equation methods. The applications of DGF in the FDTD method includes antenna simulations [2], [3], FDTD simulations on disjoint domains [9], DGF-FDTD hybrid simulations [10] and absorbing boundary conditions for FDTD [4].

Until recently, multiple-precision arithmetic (MPA) [11] has been required for the DGF generation, which consumes large computing resources in terms of processor time and memory. Therefore, possibilities for the DGF generation with the use

of the recurrence schemes are investigated. Recently, such recurrence schemes [12], [13] have been proposed. Using the creative-telescoping technique implemented in a symbolic mathematics software, the recurrence schemes are obtained without deep understanding of mathematical functions behind it. Moreover, these results are obtained for the magic time-step size [1] only, which is not treated as stable in real simulations [14], [15]. Usually, the time-step size is slightly reduced below the Courant stability limit (e.g., by multiplying limiting value of the time-step size by 0.99) to avoid stability issues in practical simulations.

In [16], we derive the no-neighbours recurrence scheme for one-dimensional (1-D) FDTD-compatible DGF using solely properties of the Gauss hypergeometric function (GHF). Scalar DGF is represented by GHF and using known properties of GHF, the recurrence scheme is obtained for arbitrary stable time-step size. In this paper, we evaluate accelerations of FDTD computations that are possible to obtain with the use of our recurrence scheme. Although 2- and 3-D recurrence schemes for DGF (valid not only for the magic time-step size) still need to be derived, the 1-D case represents the starting point for any research in this area.

II. DGF-FDTD METHOD

Let us consider the 1-D wave propagation along the z direction in the FDTD mesh. DGF allows one to represent 1-D FDTD update equations with the use of the convolution formulation

$$\begin{bmatrix} E_k^n \\ H_k^n \end{bmatrix} = \sum_{n',k'} \begin{bmatrix} G_{ee}^{n-n'} & G_{eh}^{n-n'} \\ G_{he}^{n-n'} & G_{hh}^{n-n'} \end{bmatrix} \cdot \begin{bmatrix} J_{k'}^{n'} \\ M_{k'}^{n'} \end{bmatrix} \quad (1)$$

where E and H denote respectively electric- and magnetic-field vectors, J and M denote respectively electric- and magnetic-current source vectors, and n and k denote respectively temporal and spatial indices of the FDTD mesh. G_{ee} ,

G_{eh} , G_{he} , G_{hh} functions can be obtained for the free space as follows:

$$\begin{aligned} G_{ee_k}^n &= -\frac{\Delta t}{\epsilon_0} (g_k^n - g_k^{n-1}) \\ G_{eh_k}^n &= \Delta z \gamma^2 (g_k^n - g_{k-1}^n) \\ G_{he_k}^n &= \Delta z \gamma^2 (g_{k+1}^n - g_k^n) \\ G_{hh_k}^n &= -\frac{\Delta t}{\mu_0} (g_k^{n+1} - g_k^n) \end{aligned} \quad (2)$$

where ϵ_0 and μ_0 denote respectively permittivity and permeability of the free space, and Δt and Δz denote respectively temporal- and spatial-step size. 1-D scalar DGF can be computed with the use of the following formula [8]:

$$g_k^n = \sum_{m=k}^{n-1} \gamma^{2m} \binom{m+n}{2m+1} \binom{2m}{m+k} (-1)^{m+k} \quad (3)$$

where $\gamma = \frac{c\Delta t}{\Delta z}$ ($c = (\sqrt{\mu_0\epsilon_0})^{-1}$) denotes the Courant number that must be less than or equal to one ($\gamma \leq 1$) to guarantee stability of computations. Scalar DGF (3) requires MPA computations for large indices in binomial coefficients, hence applicability of this formula is limited.

III. RECURRENCE SCHEME

Taking into consideration the formula (2) for calculation of $G_{ee_k}^n$ and scalar DGF formula (3), one obtains

$$\begin{aligned} G_{ee_k}^n &= -\gamma^{2k} \frac{\Delta t}{\epsilon_0} \left(\sum_{j=0}^{n-k-1} (-1)^j \gamma^{2j} \binom{n+k+j-1}{2k+2j} \binom{2k+2j}{2k+j} \right) \\ &= -\gamma^{2k} \frac{\Delta t}{\epsilon_0} \left(\sum_{j=0}^{n-k-1} \frac{(-\gamma^2)^j}{j!} \frac{(n-1+k+j)!}{(n-k-1-j)!(2k+j)!} \right) \\ &= -\gamma^{2k} \frac{\Delta t}{\epsilon_0} \frac{(n+k-1)!}{(n-k-1)!(2k)!} \left(\sum_{j=0}^{n-k-1} \frac{(\gamma^2)^j}{j!} \frac{(n+k)_j (k-n+1)_j}{(2k+1)_j} \right) \\ &= -\gamma^{2k} \frac{\Delta t}{\epsilon_0} \frac{(n+k-1)!}{(n-k-1)!(2k)!} \times \\ &\quad {}_2F_1(n+k, k-n+1, 2k+1; \gamma^2) \end{aligned} \quad (4)$$

where $(z)_j = z \cdot (z+1) \cdot \dots \cdot (z+j-1)$ denotes the Pochhammer symbol (see Formula (1.5) in [17]) and ${}_2F_1(a, b, c; z)$ denotes GHF [17].

Our aim is to employ Gauss contiguous relations [18] to (4). According to [19] and [20], one can find a linear relation between any three contiguous hypergeometric functions. Hence, one obtains

$$\begin{aligned} &\frac{b(c-a)}{(a-1-b)} {}_2F_1(a-1, b+1, c; z) + \\ &\frac{a(c-b)}{(a+1-b)} {}_2F_1(a+1, b-1, c; z) + \\ &\left(c-2a + (a-b)z + \frac{a(a+1-c)}{(a+1-b)} + \frac{(a-1)(a-c)}{(a-1-b)} \right) \times \\ &\quad {}_2F_1(a, b, c; z) = 0. \end{aligned} \quad (5)$$

We are interested in values of ${}_2F_1(n+k, k-n+1, 2k+1; \gamma^2)$ for fixed $k \in \mathbb{Z}$, hence the above relation is transformed into

the formula with $z = \gamma^2$, $a = n+k$, $b = k-n+1$ and $c = 2k+1$

$$\begin{aligned} &\frac{(k-n+1)^2}{(2n-2)} g(n-1) + \frac{(n+k)^2}{2n} g(n+1) + \\ &\left(1-2n + (2n-1)\gamma^2 + \frac{(n+k)(n-k)}{2n} + \right. \\ &\quad \left. \frac{(n+k-1)(n-k-1)}{(2n-2)} \right) g(n) = 0. \end{aligned} \quad (6)$$

Taking into account that

$$g(n) = -G_{ee_k}^n \gamma^{-2k} \frac{\epsilon_0}{\Delta t} \frac{(n-k-1)!(2k)!}{(n+k-1)!} \quad (7)$$

one obtains the recurrence scheme as follows:

$$\begin{aligned} G_{ee_k}^n &= -\frac{(n-k-2)(n-1)(n+k-2)}{(n-2)(n+k-1)(n-k-1)} G_{ee_k}^{n-2} \\ &- \left(\frac{2(n-1)(3-2n)}{(n+k-1)(n-k-1)} + \frac{2(n-1)(2n-3)}{(n+k-1)(n-k-1)} \gamma^2 + 1 \right. \\ &\quad \left. + \frac{(n-1)(n+k-2)(n-k-2)}{(n-2)(n+k-1)(n-k-1)} \right) G_{ee_k}^{n-1}. \end{aligned} \quad (8)$$

The initial values for the recurrence may be found directly from (2), (3) for $n = k+1$ and $n = k+2$ as

$$G_{ee_k}^{k+1} = -\gamma^{2k} \frac{\Delta t}{\epsilon_0} \quad (9)$$

$$G_{ee_k}^{k+2} = -\gamma^{2k} \frac{\Delta t}{\epsilon_0} \left(2k+1 - (2k+2)\gamma^2 \right). \quad (10)$$

Eq. (8) enables fast generation of time-domain G_{ee} waveforms for fixed spatial position k . Using (2), the scalar DGF waveform and dyadic DGF components (i.e., G_{eh} , G_{he} , G_{hh}) can be computed.

IV. NUMERICAL RESULTS

Codes implementing DGF generation with the use of the formula (3) requiring MPA computations, the recurrence scheme (8) and the direct FDTD method are developed in C programming language. Final results of computations are obtained in double floating-point precision. Benchmarks are executed on a single Intel i7 core (i7-7700 CPU @ 3.60GHz). In the presented results, Courant number is set to $\gamma = 0.9$. Numerical results are presented for varying position k of an observation point and DGF waveform length L . Since the value of the scalar DGF waveform is equal to zero up to $n = k+1$, L denotes the waveform length after wavefront arrival to the observation point. That is, the total FDTD simulation time is set to $k+L$ for the DGF generation in our benchmarks. In the FDTD reference computations, the position of the source exciting the domain is set to $k=0$ and the FDTD domain is symmetrical. Furthermore, the length of the domain in the FDTD reference computations is minimal allowing us to avoid reflections from domain boundaries in simulation results. For DGF generation with the use of formula (3) requiring MPA, the precision of the floating-point computations is set to 4096 bits.

In Fig. 1(a), the electric field E is presented for excitation of the FDTD mesh with the use of the harmonic current source J_0^n (frequency set to 3.175 GHz). The results are computed as



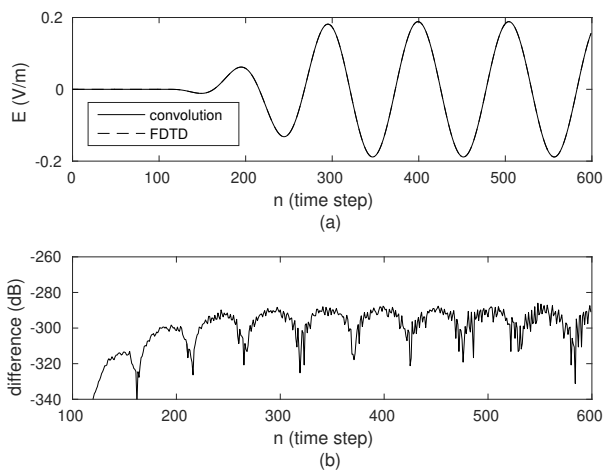


Fig. 1. Simulation results ($k = 100$, $L = 500$) for FDTD and DGF-FDTD: (a) waveforms, (b) numerical error.

the convolution of the source with DGF and using the direct FDTD method for sufficiently long domain. The observation point and the waveform length are respectively set to $k = 100$ and $L = 500$. The obtained waveforms closely overlap, hence, the difference between both waveforms is studied in detail in Fig. 1(b). As seen, the difference is around the numerical noise level (-300 dB), which confirms the correctness of the developed codes.

In Fig. 2, computing times are presented for the generation of G_{ee} DGF with the use of the formula (3) requiring MPA, the recurrence scheme (8) and the direct FDTD method. In this benchmark, the position of observation point is set to (a) $k = 100$, (b) $k = 300$, (c) $k = 500$ whereas the length of the DGF waveform L is varied. In all cases, the time of the DGF generation increases when the waveform length is increased. However, the increase of computing times is the highest for the formula (3) requiring MPA computations and approaches three orders of magnitude of CPU time for the DGF waveform length increased from $L = 40$ to $L = 500$. The CPU-time requirement is the lowest for the recurrence scheme (8) because it does not include overhead related to computations before the wave-front arrival to the observation point ($n < k$). For the considered cases (a)–(c), the generation of the DGF waveform with the use of the recurrence scheme (8) is two/three orders of magnitude faster than the direct FDTD method.

In Fig. 3, G_{ee} DGF computing times are presented for varying position of the observation point k and the length of the DGF waveform set to (a) $L = 300$, (b) $L = 400$, (c) $L = 500$. For the direct FDTD method, the computing time increases when the distance from source k is increased. It stems from increase of the FDTD domain size required to generate DGF without reflections from boundaries. On the other hand, the DGF generation methods based on the formula (3) and the recurrence scheme (8) require constant processor time when the position of observation point k is varied. For

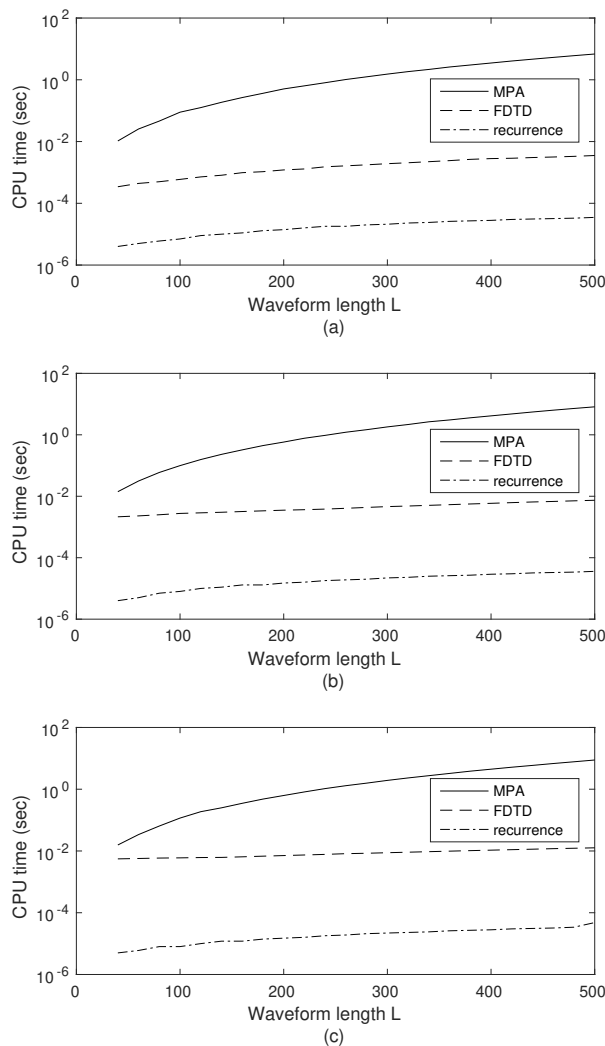


Fig. 2. DGF computation times for (a) $k = 100$, (b) $k = 300$, (c) $k = 500$ and varying length of the DGF waveform L .

the considered 1-D cases (a)–(c), the generation of the DGF waveform with the use of the recurrence scheme (8) is two orders of magnitude faster than the direct FDTD method and four orders of magnitude faster than the method based on formula (3) requiring MPA.

In the next benchmarks, electric fields are computed for excitation of the FDTD mesh with the use of the harmonic current source J_0^n (frequency set to 3.175 GHz). The results are computed as the convolution of the source with DGF and using the direct FDTD method. DGF is computed with the use of the recurrence scheme (8). In Fig. 4, computing times are presented for the computation of electric field in the FDTD mesh when the position of observation point is set to (a) $k = 100$, (b) $k = 300$, (c) $k = 500$ and the length of the DGF

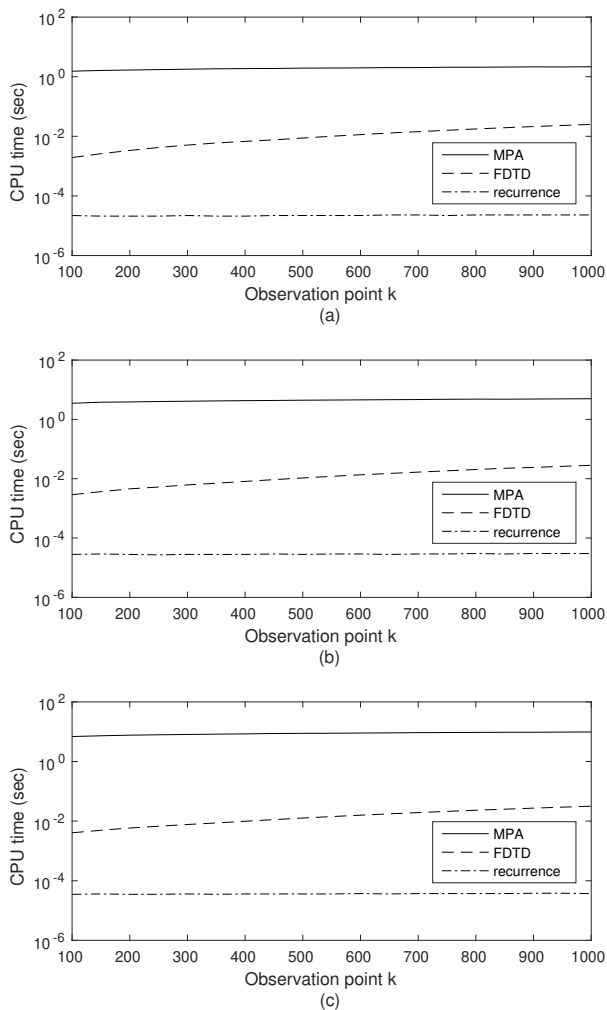


Fig. 3. DGF computation times for (a) $L = 300$, (b) $L = 400$, (c) $L = 500$ and varying position of observation point k .

waveform L is varied. In Fig. 5, computing times are presented for varying position of observation point k whilst the length of the DGF waveform is set to (a) $L = 300$, (b) $L = 400$, (c) $L = 500$. In these benchmarks, the method based on the recurrence scheme is around a single order of magnitude faster than the direct FDTD method. This acceleration results mainly from the FDTD overhead related to computations before the wave-front arrival to the observation point ($n < k$). Although convolution computations slow down DGF-FDTD, it is still possible to obtain FDTD-compatible simulation results faster than by using direct FDTD.

V. CONCLUSION

In this paper, a new approach to the generation of the 1-D FDTD-compatible DGF is presented that employs recurrence

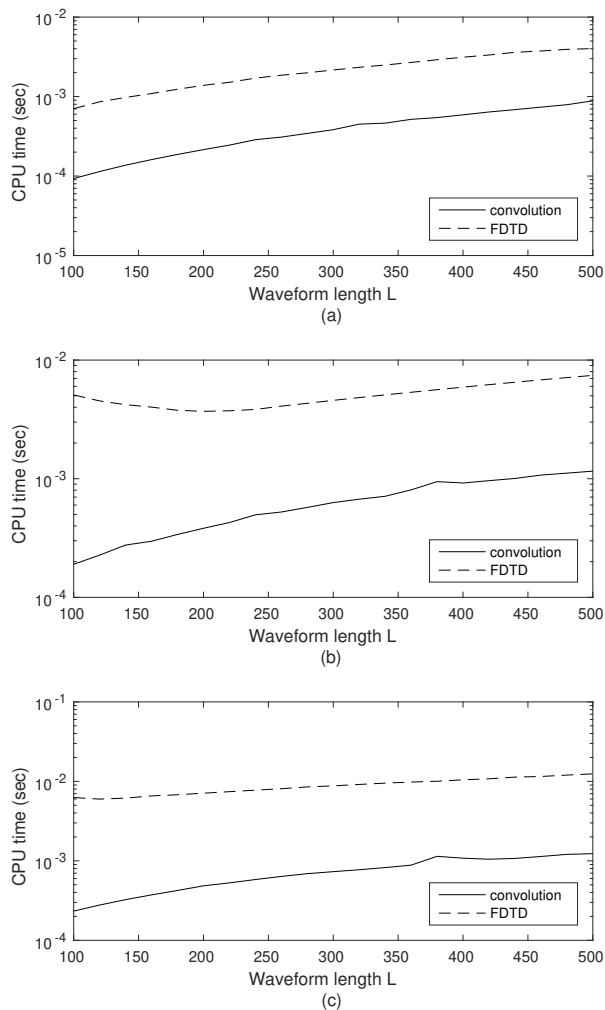


Fig. 4. Computation times for (a) $k = 100$, (b) $k = 300$, (c) $k = 500$ and varying length of the DGF waveform L .

scheme. It is valid not only for the magic time-step size but also for an arbitrary stable value of the Courant number. Computations of 1-D FDTD solutions with the use of the DGF-FDTD method can be around an order of magnitude faster than those based on the direct FDTD method. Our further research steps are directed towards the DGF generation in the 2-D case.

REFERENCES

- [1] A. Taflov and S. C. Hagness, *Computational Electrodynamics: The Finite-difference Time-domain Method*, 3rd edition, Artech House, Boston, 2005.
- [2] J. Vazquez, C. G. Parini, "Discrete Green's function formulation of FDTD method for electromagnetic modelling," *Electron. Lett.*, vol. 35, no. 7, pp. 554–555, 1999.

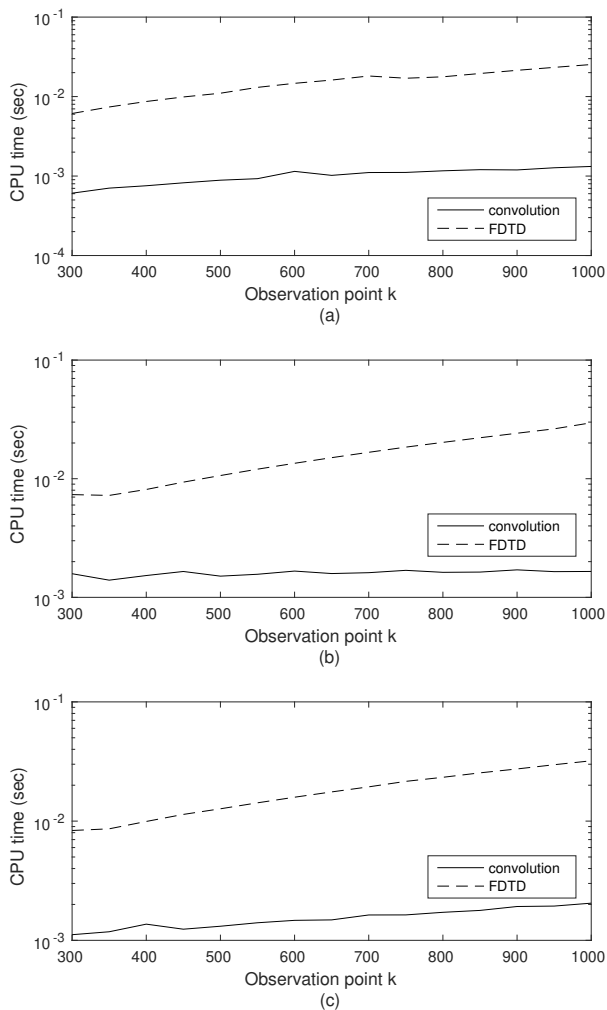


Fig. 5. Computation times for (a) $L = 300$, (b) $L = 400$, (c) $L = 500$ and varying position of observation point k .

- [3] W. Ma, M. R. Rayner, C. G. Parini, "Discrete Green's function formulation of the FDTD method and its application in antenna modeling," *IEEE Trans. Antennas Propag.*, vol. 53, no. 1, pp. 339–346, 2005.
- [4] R. Holtzman, R. Kastner, E. Heyman, and R. W. Ziolkowski, "Stability analysis of the Green's function method (GFM) used as an ABC for arbitrarily shaped boundaries," *IEEE Trans. Antennas Propag.*, vol. 50, no. 7, pp. 1017–1029, 2002.
- [5] R. Kastner, "A multidimensional Z-transform evaluation of the discrete finite difference time domain Green's function," *IEEE Trans. Antennas Propag.*, vol. 54, no. 4, pp. 1215–1222, 2006.
- [6] N. Rospsha, R. Kastner, "Closed form FDTD-compatible Green's function based on combinatorics," *J. Computat. Phys.*, vol. 226, no. 1, pp. 798–817, 2007.
- [7] S.-K. Jeng, "An analytical expression for 3-D dyadic FDTD-compatible Green's function in infinite free space via Z-transform and partial difference operators," *IEEE Trans. Antennas Propag.*, vol. 59, no. 4, pp. 1347–1355, 2011.
- [8] T. P. Stefański, "A new expression for the 3-D dyadic FDTD-compatible Green's function based on multidimensional Z-transform," *IEEE Antennas Wirel. Propag. Lett.*, vol. 14, pp. 1002–1005, 2015.
- [9] T. P. Stefański, "Discrete Green's function approach to disjoint domain simulations in 3D FDTD method," *Electron. Lett.*, vol. 49, no. 9, pp. 597–598, 2013.
- [10] T. P. Stefański, "Hybrid technique combining the FDTD method and its convolution formulation based on the discrete Green's function," *IEEE Antennas Wirel. Propag. Lett.*, vol. 12, pp. 1448–1451, 2013.
- [11] T. P. Stefański, "Electromagnetic problems requiring high-precision computations," *IEEE Antennas Propag. Mag.*, vol. 55, no. 2, pp. 344–353, 2013.
- [12] B. P. de Hon, J. M. Arnold, "Recursive evaluation of space-time lattice Green's functions," *J. Phys. A: Math. Theor.*, vol. 45, 385202, 2012.
- [13] B. P. de Hon, S. J. Floris, J. M. Arnold, "No-neighbours recurrence schemes for space-time Green's functions on a 3D simple cubic lattice," *J. Phys. A: Math. Theor.*, vol. 51, 085201, 2018.
- [14] M. S. Min, C. H. Teng, "The instability of the Yee scheme for the "magic time step"," *J. Computat. Phys.*, vol. 166, no. 2, pp. 418–424, 2001.
- [15] R. F. Remis, "On the stability of the finite-difference time-domain method," *J. Computat. Phys.*, vol. 163, no. 1, pp. 249–261, 2000.
- [16] J. Gulowski, T. P. Stefański, "Recurrence scheme for FDTD-compatible discrete Green's function derived based on properties of Gauss hypergeometric function," *Journal of Electromagnetic Waves and Applications*, pp. 1–17, DOI 10.1080/09205071.2019.1568308, 2019.
- [17] W. Koepf, *Hypergeometric Summation*, Springer-Verlag, London, 2014.
- [18] H. Bateman, *Higher Transcendental Functions Vol. I-III.*, McGraw-Hill Book Company, New York, 1953.
- [19] R. Vidunas, "Contiguous relations of hypergeometric series," *J. Comp. Appl. Math.*, vol. 153, pp. 507–519, 2003.
- [20] A. K. Ibrahim, M. A. Rakha, "Contiguous relations and their computations for ${}_2F_1$ hypergeometric series," *Comput. Math. Appl.*, vol. 56, pp. 1918–1926, 2008.